

# Statistics of polarization dependent loss in an installed long-haul WDM system

Lynn E. Nelson,<sup>1,\*</sup> Cristian Antonelli,<sup>2</sup> Antonio Mecozzi,<sup>2</sup> Martin Birk,<sup>1</sup> Peter Magill,<sup>1</sup>  
Anton Schex,<sup>3</sup> and Lutz Rapp<sup>3</sup>

<sup>1</sup>AT&T Labs – Research, 200 S. Laurel Avenue, Middletown, New Jersey 07748, USA

<sup>2</sup>University of L'Aquila, L'Aquila, Italy

<sup>3</sup>Nokia Siemens Networks, Munich, Germany

\*lenelson@research.att.com

**Abstract:** We have made continual, multiple-day measurements of the polarization dependent loss of multiple C-band channels in an installed 1800 km terrestrial link. The PDLs of individual channels varied on the time-scale of hours, while the temporal variations of the PDLs of adjacent channels often tracked. The probability densities of the field measurements of PDL were not Maxwellian and instead were truncated, consistent with the limited number of elements in the link having appreciable PDL. A new model for the statistics of PDL in systems with few PDL elements is proposed, where a lower bound of the distribution exists if there is a dominant PDL element. The probability distributions from measurement and theory show good agreement.

©2011 Optical Society of America

**OCIS codes:** (060.2330) Fiber optics communications; (260.5430) Polarization; (060.2360) Fiber optics links and subsystems.

---

## References and links

1. H. Sun, K.-T. Wu, and K. Roberts, "Real-time measurements of a 40 Gb/s coherent system," *Opt. Express* **16**(2), 873–879 (2008).
2. L. E. Nelson, S. L. Woodward, S. Foo, X. Zhou, M. D. Feuer, D. Hanson, D. McGhan, H. Sun, M. Moyer, M. O. Sullivan, and P. D. Magill, "Performance of a 46-Gbps dual-polarization QPSK transceiver with real-time coherent equalization over high PMD fiber," *J. Lightwave Technol.* **27**(3), 158–167 (2009).
3. T. Duthel, C. R. S. Fludger, J. Geyer, and C. Schülien, "Impact of polarisation dependent loss on coherent PolMux-NRZ-DQPSK," in *Proc. OFC-NFOEC 2008*, Feb. 24–28, 2008, San Diego, CA, paper OThU5.
4. O. Vassilieva, T. Hoshida, X. Wang, J. Rasmussen, H. Miyata, and T. Naito, "Impact of polarization dependent loss and cross-phase modulation on polarization-multiplexed DQPSK signals," in *Proc. OFC-NFOEC 2008*, Feb. 24–28, 2008, San Diego, CA, paper OThU6.
5. C. Xie, "Polarization-dependent loss induced penalties in PDM-QPSK coherent optical communication systems," in *Proc. OFC-NFOEC 2010*, March 21–25, 2010, San Diego, CA, paper OWE6.
6. M. Shtaif, "Performance degradation in coherent polarization multiplexed systems as a result of polarization dependent loss," *Opt. Express* **16**(18), 13918–13932 (2008).
7. J. Jiang, D. Richards, C. Allen, S. Oliva, and R. Hui, "Non-intrusive polarization dependent loss monitoring in fiber-optic transmission systems," *Opt. Commun.* **281**(18), 4631–4633 (2008).
8. J. Jiang, D. Richards, S. Oliva, P. Green, and R. Hui, "PMD and PDL monitoring of traffic-carrying transatlantic fibre-optic system," *Electron. Lett.* **45**(2), 123–124 (2009).
9. L. E. Nelson, M. Birk, P. Magill, A. Schex, and L. Rapp, "Measurements of the polarization dependent loss of multiple WDM channels in an installed, long-haul terrestrial link," in *IEEE Photonics Society Summer Topical 2010*, 19–21 July 2010, Playa del Carmen, Mexico, paper MA3.4.
10. A. Mecozzi and M. Shtaif, "The statistics of polarization-dependent loss in optical communication systems," *IEEE Photon. Technol. Lett.* **14**(3), 313–315 (2002).
11. C. Hentschel and D. Derickson, in *Fiber Optic Test and Measurement*, (Prentice Hall, 1998), p. 355.
12. N. Bergano, in *Optical Fiber Telecommunications IVB* (Academic Press, 2002), p. 183.
13. M. Brodsky, M. Boroditsky, P. Magill, N. J. Frigo, and M. Tur, "Persistence of spectral variations in DGD statistics," *Opt. Express* **13**(11), 4090–4095 (2005).
14. A. Mecozzi, C. Antonelli, M. Boroditsky, and M. Brodsky, "Characterization of the time dependence of polarization mode dispersion," *Opt. Lett.* **29**(22), 2599–2601 (2004).
15. M. Brodsky, N. J. Frigo, M. Boroditsky, and M. Tur, "Polarization mode dispersion of installed fibers," *J. Lightwave Technol.* **24**(12), 4584–4599 (2006).
16. Y. Fukada, "Probability density function of polarization dependent loss (PDL) in optical transmission systems composed of passive devices and connecting fibers," *J. Lightwave Technol.* **20**(6), 953–964 (2002).

17. C. Antonelli and A. Mecozzi, "Statistics of the DGD in PMD emulators," *IEEE Photon. Technol. Lett.* **16**(8), 1840–1842 (2004).
  18. N. Gisin, "Statistics of polarization dependent losses," *Opt. Commun.* **114**(5-6), 399–405 (1995).
  19. M. Shtaif and A. Mecozzi, "Study of the frequency autocorrelation of the differential group delay in fibers with polarization mode dispersion," *Opt. Lett.* **25**(10), 707–709 (2000).
- 

## 1. Introduction

Recent research and development has focused on coherent detection and digital signal processing (DSP), particularly for the polarization-division-multiplexed (PDM) quadrature-phase-shift-keyed modulation format [1], to meet the demands for 40 Gb/s and 100 Gb/s line rates. In addition to the promise of high spectral efficiency, coherent transponders using DSP offer several advantages to carriers, including high tolerance to chromatic dispersion [1] and polarization mode dispersion (PMD) [2], permitting operation over a variety of fiber types, vintages, and ranges of fiber parameters.

Polarization dependent loss (PDL), on the other hand, is proving to be a more challenging impairment for coherent systems, particularly those employing numerous reconfigurable add-drop multiplexers (ROADMs), since the DSP cannot completely compensate the effects of PDL on a PDM signal. Prior measurements [3,4], simulations [5], and theoretical studies [6] have elucidated the effects of PDL on PDM signals: a single PDL element causes a power/optical signal-to-noise ratio (OSNR) difference of the two polarization tributaries and/or non-orthogonality of the (originally orthogonal) polarization tributaries, depending on the relative orientation of the polarization tributaries to the PDL axis. A PDM signal in a system with multiple amplified spans and multiple, randomly oriented PDL elements will incur both impairments. Although DSP can effectively separate the tributaries even in the presence of non-orthogonality [1], DSP is not able to compensate the degraded OSNR of one of the polarization tributaries.

To date, while the effects of PDL on PDM signals have been characterized, much less has been known about the actual PDL of installed long-haul systems with multiple spans and amplifiers, due to a dearth of field measurements. Exceptions are [7,8], where a coherent receiver was used to measure the PDL component parallel to the local oscillator polarization, and [9]. Estimates of link PDLs generally have been based on [10], which asserts that, for low PDL resulting from many contributions distributed along the link (where mean PDL is less than 8 dB), the accumulated PDL is a Maxwell-distributed random variable, when expressed in decibels. The mean-square PDL value then would be equal to the sum of the mean-square values of the individual PDL contributions. Using the presumed Maxwellian distribution for PDL and assuming dynamics that explore the whole distribution in less than a year, system vendors generally base their link engineering rules on requiring transponders to tolerate three times the expected mean accumulated PDL to ensure a sufficiently low outage probability. If the PDL of the individual components are overestimated due to measurement inaccuracies/conservatism and/or the statistics of the accumulated PDL is not Maxwellian, the result could be engineering rules having more than the intended margin and shorter regenerator spacing, at higher cost to the carrier. As a follow-up to [9], here we provide a more comprehensive report of the results of continuous, multiple-day PDL measurements of an installed, long-haul terrestrial link. In addition, we outline a new model for the statistics of PDL in systems with few PDL elements, and we show good agreement of measured and modeled probability densities for PDL.

## 2. Measurements of PDL in the field

PDL measurements were conducted over a portion of AT&T's ultra-long-haul network between Florida and Louisiana. An existing 900 km link optimized for 10 Gb/s and 40 Gb/s transmission on a 50 GHz spaced grid was looped back to form an 1800 km optical link. The 900 km link consists of twelve spans of standard single-mode fiber (G.652, SSMF) with erbium-doped fiber amplifiers (EDFA) and fiber-based dispersion compensating modules (DCF) at each EDFA's mid-stage to compensate ~96% of the dispersion of each span. The average span length and loss were 78 km and 16.5 dB, respectively. The average PMD of the

transmission fiber was  $0.03 \text{ ps}/(\text{km}^{1/2})$ , and the DCFs each had an average PMD of 0.35 ps. The WDM channels passed through six ROADMs: a pair in Ellisville, FL added the channels at the transmitter and dropped the channels at the receiver, a pair in New Orleans, LA dropped and then added the channels (connected via fiber jumpers) at the loop-back, and ROADMs after eight and 16 spans expressed the channels. Figure 1 shows a schematic of the system.

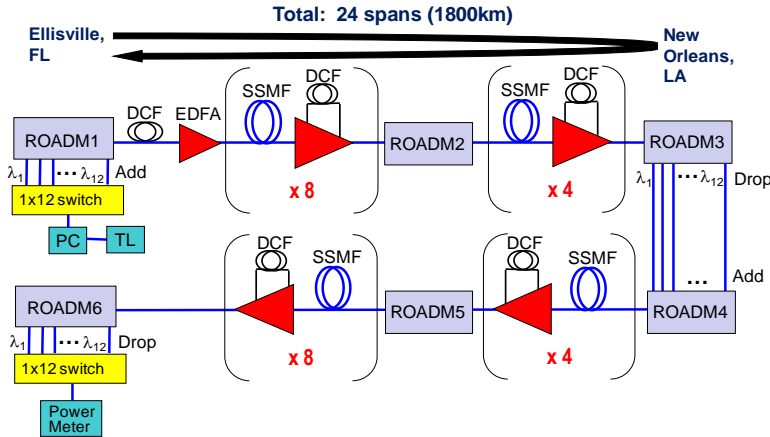


Fig. 1. Schematic of transmission system and apparatus for measuring PDL of multiple WDM channels. The twelve measurement channels are denoted as  $\lambda_1$  to  $\lambda_{12}$ . Not shown in the figure are ten WDM loading channels, distributed across the C-band, which also were added at ROADM1 and transmitted over the 1800 km looped-back link.

## 2.1 Measurement procedure

The system was loaded with ten WDM channels (nine continuous-wave DFB lasers and one 10 Gb/s transponder) that were fairly evenly distributed across the C-band. A tunable laser served as the channel-under-test and could be switched among twelve available channels (191.70, 191.75, 191.85, 191.90, 192.85, 192.90, 192.95, 193.0, 194.40, 194.45, 194.55, and 194.60 THz) at system input. We attempted several PDL measurement techniques and settled on the All States method [11], implemented asynchronously, due to the system control loops and the  $\sim 10$  msec delay of the 1800 km transmission. A fast polarization controller (PC) following the tunable laser (TL) repeatedly launched a sequence of 1000 random polarization states covering the Poincare sphere at a 10 kHz rate, the highest polarization switching speed allowed by the measurement apparatus and faster than the minimum of 7 kHz recommended in [12] to minimize polarization hole burning (PHB). As shown in Fig. 1, after the 1800 km transmission the channel-under-test was dropped at the final ROADM, and its power was measured using a 1x12 optical switch and fast power meter. PDL was calculated from the ratio of the maximum and minimum powers of the channel-under-test as the launch polarization was switched, measured within a 1 sec window, with 10  $\mu$ sec averaging on the power meter. To verify reproducibility, twenty such PDL measurements were made, each with a different random sequence of 1000 polarization states. The 20 measurements were then averaged to obtain the PDL for the channel.

The tunable laser was then switched to the next measurement channel, and the system control loops were allowed to stabilize the channel power levels before again measuring PDL. Since it took nearly 1.5 hours to serially measure all twelve channels due to the time required for switching channels and system stabilization, we measured various groups of four channels, instead of measuring all twelve channels during a particular measurement set. The “cycle time” to serially measure four channels was 27 minutes. Due to the system’s power stability, over the 1 sec measurement window, the minimum PDL that could be measured was 0.25 dB.

## 2.2 Measurement results

Figure 2 shows the PDL variation over time for a set of four C-band channels. The mean PDL over all measurements of all twelve channels was 1.50 dB, agreeing well with the calculated estimate of 1.5 dB for the 1800 km link's mean PDL based on the sum of the mean-square values of the expected mean PDL of the ROADMs (nominally, 0.4dB for express or add paths, and 0.8dB for drop paths) and polarization-dependent gain (PDG) of the EDFAs (<0.1dB per EDFA). In Fig. 2, the 1540 nm channels (194.45 and 194.55 THz) have mean PDLs of 1.70 and 1.66 dB, respectively, which are among the highest of all measured channels; whereas the 1550 nm channels (193.00 and 192.90 THz) have mean PDLs of 1.37 and 1.29 dB, among the lowest of all measured channels. Figure 2 shows that the PDLs of the 1550 nm (1540 nm) channels track each other over certain time periods, as could be expected based on wavelength-independent component PDLs and the low PMD of the link (2.1 ps). Note that the PDL of two channels near 1530 nm (196.00 and 195.95 THz) also were measured [9]; however, the mean PDLs were ~3.5 dB, significantly higher than the calculated estimate of 1.9 dB for these channels. We attribute the large PDL near 1530 nm to PHB in the EDFAs [9], which was not significant for the other twelve measurement channels. Therefore, PDL measurements at 196.00 and 195.95 THz were not included in this paper.

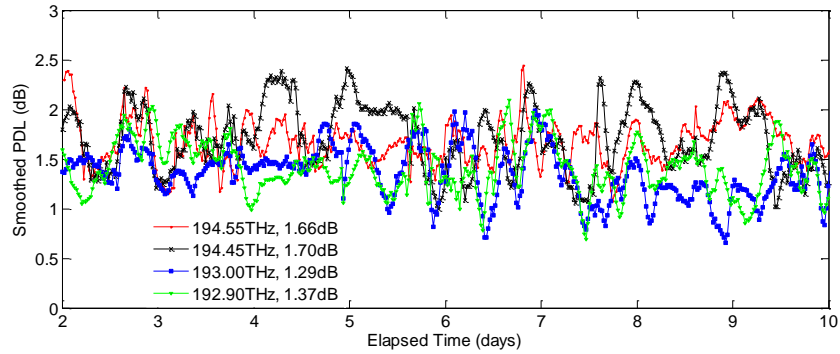


Fig. 2. Measured PDL of the 1800 km loop-back link for four channels. Legends show mean PDLs of the channels over 15 days.

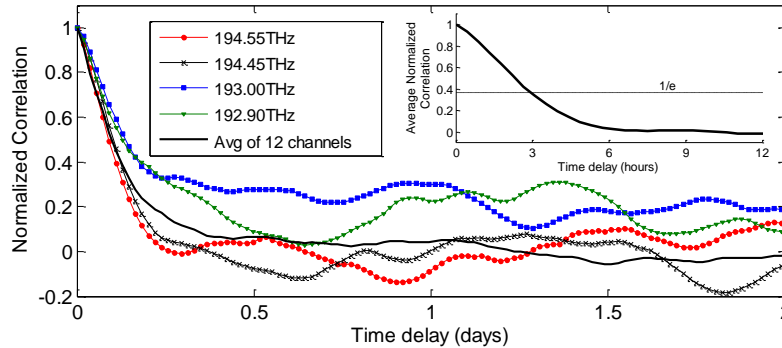


Fig. 3. Normalized autocorrelations of the PDL –  $\langle \text{PDL} \rangle$  for the four channels shown in Fig. 2 as a function of time delay. Solid curve is the average of the normalized autocorrelations for all 12 channels included in the histograms in Fig. 4 and is also shown in the inset.

Figure 3 shows normalized autocorrelations as a function of time delay for the PDL measurements shown in Fig. 2. Measurements of the other channels showed similar correlation times. Also shown is the average of the normalized autocorrelations of the PDLs of all twelve channels considered in this paper. The average autocorrelation drops to  $1/e$  at  $\tau_{\text{corr}} \approx 3$  hours. Assuming an exponential decay of the correlation function, over the  $T = 15$

days of measurements in Fig. 2, the number of independent samples in each PDL time series is therefore the observation time divided by the width of the two-sided correlation function, that is  $T/(2 \tau_{\text{corr}}) \sim 60$ .

### 3. Model of truncated PDL

The hinge model for PMD [13] assumes that the PMDs of the buried sections of installed fibers are frequency *dependent* yet fixed (over some time scale), and the hinges, which model the components (jumpers, etc.) at the amplifier huts, randomly vary in time in response to environmental perturbations. The analysis of this model reveals that the temporal statistics of the differential group delay (DGD) is characterized by a truncated distribution [14], although the full theoretical characterization of the temporal statistics is limited by the fact that the hinge rotation statistics are in general anisotropic [15].

Here we extend the hinge model to PDL, assuming that *at a given time* the amplifier huts are the locations of the fixed, frequency independent PDL elements, and the transmission fibers connecting amplifier huts act as frequency-dependent rotators. A similar model, restricted to the case of identical PDL elements, was considered in [16]. In this situation, at a given time, different channels experience different fiber rotations but the same PDL elements and thus are equivalent to different realizations of the same PDL statistics. A single histogram of the data measured over many channels should hence provide the statistics of PDL over an ensemble of realizations obtained with concatenated PDL elements of fixed magnitudes and isotropically distributed axes. In addition, the PDL of each channel still experiences a random variation in time caused by the jumpers at amplifiers huts, which act as time dependent and frequency independent (in general anisotropic) rotators. In this framework, measuring the PDLs of multiple channels over a time interval longer than the PDL correlation time, gives access to different sets of independent realizations of the same ensemble statistics.

If instead of considering the time-frequency statistics of PDL, one considers the time-frequency statistics of the DGD, the result would be a Maxwellian distribution, because the individual PMD elements are frequency dependent and their DGDs span a Maxwellian distribution when frequency varies. An important difference between the temporal statistics of PMD and the time-frequency statistics of PDL is that the time-frequency statistics of PDL may be accurately predicted, because the rotations performed by the fiber sections are isotropic when frequency varies over a range much wider than the correlation bandwidth of the PMD vector. As noted previously, hinge rotations are generally anisotropic for PMD [15].

In Fig. 4(a)–4(d) we plot the histograms of the PDL measurements separately for the six odd and the six even channels based on 3882 and 4500 points, respectively, on linear and logarithmic scales. These histograms effectively represent the ensemble statistics of the PDL. The statistics of the odd and even channels are analyzed separately because the ROADMs split the WDM spectrum into groups of odd and even channels, which then pass through different components. We fit the histograms using the probability density function (PDF) of [17] where the differential group delay (DGD) of the fiber sections between hinges is replaced by the PDL in dB of the lumped elements. It was verified with Monte Carlo simulations based on the PDL concatenation rule [18] that this PDF is an excellent approximation up to an average PDL of about 6 dB. Five PDL elements were considered and their magnitudes were obtained via a standard least squares fitting procedure. Of course, due to the large number of fitting parameters, many solutions of the optimization procedure exist that fit the data with comparable accuracy. When we consider more PDL elements, the optimization procedure gives negligible PDL to the elements in excess of five, giving a strong indication that five is the number of relevant PDL elements in the link. This is consistent with the observation that the most significant contribution to the PDL of the 1800km link is given by the six ROADMs, the third and the fourth of which, being connected by fiber jumpers at the loop-back and not by fiber spans, are equivalent to a single element with a PDL value equal to the concatenation of the PDLs of the two individual elements.

It is apparent that the PDFs are truncated from both ends. The upper bound is a general feature of the hinge model [14]. The lower bound indicates that one PDL element, which we

speculate to correspond to the directly-connected ROADMs, predominates over the others. Note that the lower bounds to the histograms greatly exceed 0.25 dB, which as mentioned was the minimum PDL that could be measured.

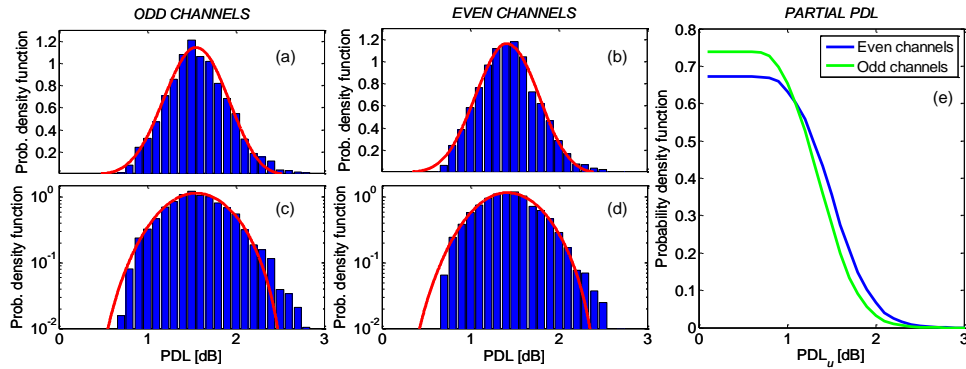


Fig. 4. Probability density functions of measured PDL along with the fits for the odd and even channels, shown on linear (a,b) and log scales (c,d). For the odd and even channels, the five PDL elements from the fit were 0.2201, 0.2432, 0.3504, 0.3519, and 1.4640 dB; and 0.2810, 0.2881, 0.3075, 0.3089, and 1.3264 dB, respectively. (e) Distribution of the axial component of PDL,  $PDL_u$ , extracted from the data of (a-d).

Although the measured odd and even channel histograms are based on a large number of points, the measured channels are not completely independent. We may approximately assume that channels are independent when their frequency difference falls outside the 3 dB bandwidth of the two-sided correlation function of the polarization rotation vector of the spans between PDL elements, thus accounting for the decorrelation of the polarization vector when frequency varies. This correlation function is difficult to evaluate, so that we may use in its place the correlation function of the PMD vector [19], which provides similar information. The two-sided bandwidth (in Hz) of this correlation function is  $\Delta B \approx 0.64/\tau_{\text{dgd}}$ . If we assume that the average DGD of a fiber link between two PDL elements is  $2.1/\sqrt{4} \approx 1.05$  ps, we obtain  $\Delta B \approx 610$  GHz. (We choose 4 here due to the locations of the ROADMs and the fiber jumpers that directly connect the two ROADMs at the loop-back.) This means that there is a good degree of correlation of the PDL fluctuations within the three groups of channels around 191, 193 and 194 THz (as is evident from Fig. 2 and in [9]), but the three groups are, mutually, fairly uncorrelated. For each channel group, we have approximately 60 independent time samples, so that the total number of independent sample points is about 180. For both odd and even channels, the ten most populated bins of the DGD distributions had between 8 and 21 independent points, so the expected fluctuation is  $\sim 1/\sqrt{21}$  to  $\sim 1/\sqrt{8}$ , about 20 to 35%.

Assuming isotropy of the PDL vector, the observed data of the PDL magnitude allow us to extract the distribution of the component of the PDL vector along a generic direction  $u$ , which is the quantity measured in [7,8]. The PDF of such a component (expressed in dB), which we denote by  $PDL_u$ , is plotted in Fig. 4(e). The presence of a lower bound in the PDF of the PDL is reflected as a flat-topped distribution near zero for  $PDL_u$ . Note however that if  $PDL_u$  is directly measured with a set-up of the kind of [7,8], this feature may be hidden by the limited statistics of the measurement, and the presence of the PDL's lower bound can be overlooked.

#### 4. Conclusion

In summary, we measured the PDL of multiple WDM channels in an installed 1800 km terrestrial link over multiple days. The PDL probability densities were truncated, consistent with the limited number of significant PDL elements in the link. We proposed a “hinge-like” model for the statistics of PDL in systems with few PDL elements, and found good agreement of probability distributions from measurement and theory.

## **Acknowledgments**

The authors gratefully acknowledge helpful discussions with Paul Wysocki and Jon Nagel.